Deciphering pH Effects on the Peptide-guided Nucleation and Growth of Hydroxyapatite and Peptide-Ion Interactions for Dentin Hypersensitivity Treatment

Yousef Mohammed Baioumy

A thesis

submitted in partial fulfillment of the

requirements for the degree of

Master of Science

University of Washington

2020

Committee:

Mehmet Sarikaya

Hanson Fong

Sami Dogan

Program Authorized to Offer Degree:

Materials Science and Engineering

University of Washington

Abstract

Deciphering pH Effects on the Peptide-guided Nucleation and Growth of Hydroxyapatite and Peptide-Ion Interactions for Dentin Hypersensitivity Treatment

Yousef Mohammed Baioumy

Chair of the Supervisory Committee:

Professor Mehmet Sarikaya

Materials Science and Engineering

With enamel demineralization being a significant factor in the development of dentinal hypersensitivity, it has been an enormous endeavor to restore the enamel. Incorporating a biomimetic approach to tooth repair has been a long-lasting challenge, especially in integrating a newly constructed mineral layer to the molecular structure of the tooth, e.g. enamel and dentin. GEMSEC's (Genetically Engineered Materials Science and Engineering Center) previous research evaluated the amelogenin-derived peptide sADP5 in guiding the remineralization of enamel and the ability to control the biomimetic mineral layer properties. Not only was remineralization achieved, but mineral integration into the tooth structure was successful in a modeled oral environment. This led to the development of a market introductory remineralizing tooth whitening dental product in the form of a lozenge as a delivery mechanism for remineralization in the oral cavity. This work was only limited to a constant saliva temperature and pH. Saliva pH is variable and dynamic and can alter hydroxyapatite crystal-growth

mechanisms. This thesis focused on the unexplored pH effects on the nucleation and growth of the newly formed mineral layer, as well as its effects on peptide characteristics, behavior, and interaction with surrounding ions. The resulting optimal pH for mineralization is used as a testing parameter in the lozenge delivered remineralization approach. Calcium assays were performed to measure the calcium consumption throughout time. Structural characterization was done using a scanning electron microscope (SEM), observing the mineral morphology, thickness, and structural integration. The results suggested that the peptide-guided nucleation and growth of the new mineral on the tooth surface can be controlled with pH. With each application of the remineralizing tooth whitening lozenge, under the pH condition determined in the pH experiments, there were clearly observable increases in the thickness of the newly formed mineral layer. The knowledge developed in this thesis will contribute to the future in everyday dental care products and change the way the oral health care system approaches treatments in periodontal diseases.

Table of Contents

List of Figures

List of Tables

Acknowledgments

Alhamdulillah, all praises and thanks to Allah, for His blessings throughout my research to complete this thesis successfully.

First and foremost, I send out my heartfelt love towards my parents, family, and friends for the immense support and encouragement, and filling my life with happiness.

I would like to express my deepest appreciation to my committee chair and advisor, Professor Mehmet Sarikaya, for the continuous support of my studies and research, motivation, and immense knowledge. He has taught me essential skills beyond the research to help me become an excellent and successful scientist. Thanks for believing in me!

I would like to also thank my close mentor, Dr. Deniz Yucesoy, for his constant guidance, encouragement, and friendship. The laboratory experiences I have learned from during my undergraduate and graduate careers were largely due to his support. I further extend my gratitude towards committee members, Drs. Hanson Fong and Sami Dogan, our close collaborators, for their invaluable clinical and scientific knowledge that heavily contributed to this research through the facilities they provided for us. Without the help of these individuals, my thesis would not have been possible.

Lastly, I would like to acknowledge the undergraduate students that I had the pleasure of mentoring during the completion of my Master's degree. Hannah Gunderman, Andy Luong, Yifei (Laura) Lyu, Sedona Sarobon, and Valerie Yuryk have been the most determined, excited, and hardest working students I have ever seen. Their support and friendship gave me comfort, and this thesis could not have been done without them.

1. Introduction – Problem Statement and Thesis Approach

1.1 Current Problem

The enamel protects the overall hierarchical structure of the tooth (**Figure 1**). The enamel is composed of 92 vol% hydroxyapatite[1].

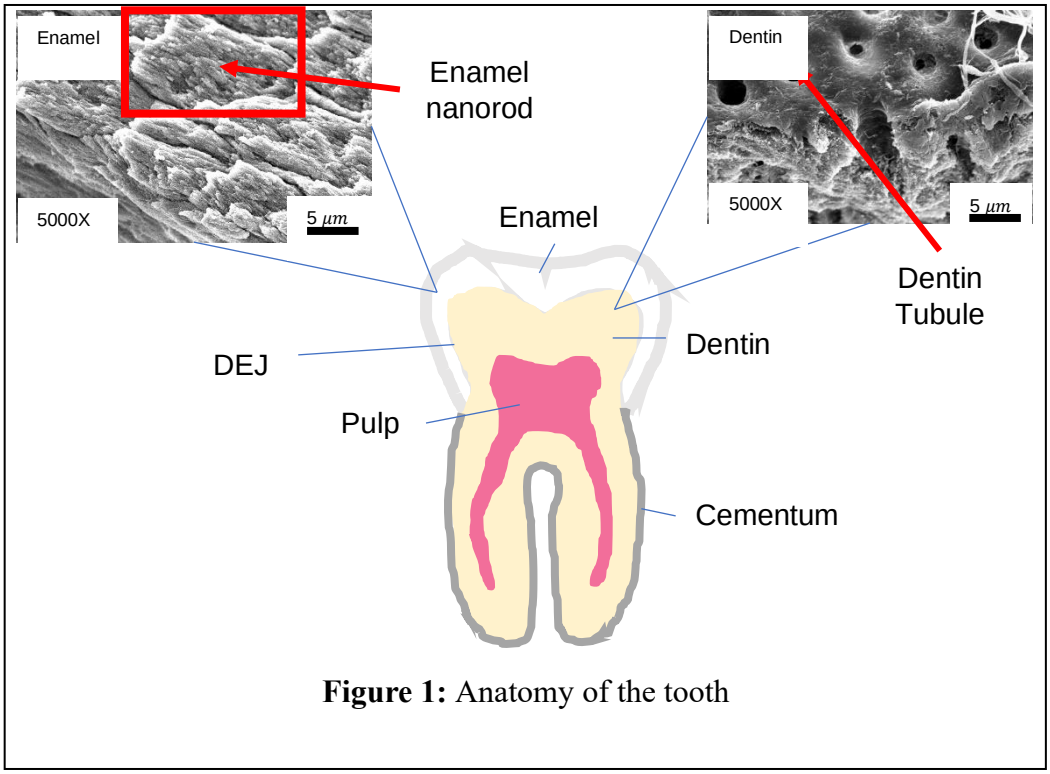

Figure 1: Anatomy of the tooth

Hydroxyapatite is a naturally occurring calcium phosphate ceramic mineral with a chemical formula of $Ca_5(PO_4)_3OH$[2,3]. Enamel is always subjected to demineralization and natural remineralization. If demineralization outweighs the remineralization, this can lead to common dental ailments such as hypersensitivity and caries. dentinal hypersensitivity is a common clinical condition that affects people of any age group and is usually associated with exposed dentin surfaces[4]. Dentin may become exposed via several means. For example, the enamel or cementum, which normally covers and protects the dentin surface, may be removed or denuded as a result of attrition, abrasion or erosion[5]. The exposure of dentin can be caused by either loss of enamel or loss of gingival tissue. Loss of gingival tissue can be caused by attachment loss due

to periodontal disease or mechanical trauma, such as over-zealous toothbrushing causing trauma to the supporting periodontal tissue[6]. Current common treatments of hypersensitivity include among others fluoride treatments, desensitization of pulpal nerves and occlusion of dental tubules[7,8].

1.2 Current Approaches for Hypersensitivity Treatment

Desensitization of pulpal nerves is a widely used approach in toothpastes for the relief of dentin hypersensitivity and utilizes potassium ions as a means of depolarizing nerve cells[9]. Sensodyne® is an example of products of this type. For the occlusion of dentin tubules, two different formulations have been used; stannous fluoride and arginine containing formulations[10,11]. Stannous fluoride (Tin (II) Fluoride) produces an occlusive layer over the surface of exposed dentin and within dentin tubules[12]. With arginine containing formulations, the hypothesis is that arginine binds to dentin with the subsequent deposition of calcium from a chalk containing formulation[13].

There are limitations to these methods. Desensitizing pulpal nerves does not provide a permanent treatment of hypersensitivity. It relieves the pain, but does not completely prevent enamel demineralization in the long term[14]. Stannous fluoride only prevents from surface demineralization. It is not effective in the subsurface lesions[15]. Arginine containing formulations lack a phosphate source and would be dependent upon sequestration of phosphate from the saliva[16].

Dental Enamel Extracellular Matrix (ECM) proteins have been used as agents to treat tooth damage caused by periodontal diseases. These proteins have been shown to have effects on cell attachment, spreading, and chemotaxis; cell proliferation and survival; expression of transcription factors; expression of growth factors, cytokines, extracellular matrix constituents,

and other macromolecules; and expression of molecules involved in the regulation of bone remodeling[17]. Traditionally, ECM proteins are associated with amelogenesis, in which ameloblasts synthesize and secrete ECM proteins including amelogenin and enamelin[18]. Amelogenin proteins play a significant role in the regulation of hydroxyapatite crystal growth during the formation of enamel. ECM protein functions go beyond enamel biomineralization. They are considered to be involved in cell differentiation for tooth crown development[19–25]. ECM proteins are also available as a therapeutic agent called Emdogain®, consisting of an enamel matrix derivative, water, and propylene glycol alginate. Emdogain® is clinically used for the periodontal regeneration of teeth affected by periodontal diseases[17]. Although Emdogain® has been used successfully for bone regeneration, there are limitations to ECM proteins due to the financial and technical challenges in the methods for obtaining these proteins[26]. Since these are not yet feasible for hypersensitivity treatment through remineralization, research has focused on developing peptides derived from the functional domains of naturally occurring proteins[26–35]. There have been many attempts made in the biomimetic remineralization of enamel, dentin, and cementum for the restoration of the tooth structure and function. These studies have included the use of full-length amelogenin[36,37], Leucine-rich amelogenin peptide[38], peptides[39,40], dendrimers[41], and physical chemistry approaches[41,42]. Though these studies influenced the motivation for tooth repair, no clinical product has become known to biomimetically remineralize the enamel *in vivo*. The methods for biomimetic tooth repair were first inspired by the successful biomineralization of hydroxyapatite using a peptide-based hydrogel containing the multifunctional peptide MDG1 (Mineral Directing Gelator)[43]. This then led to the discovery of amelogenin-derived peptides, in which the ADP5 peptide was selected for the construction of a cementum-like biomineralized microlayer to biomimetically treat periodontal diseases such as hypersensitivity[26]. Furthermore,

the ADP5 peptide has been shortened and improved to be applied in the remineralization of human enamel to treat dental carries[44].

1.3 Understanding the Hierarchical Structure of the Tooth

To successfully carry out a biomimetic approach to tooth repair, the structure and function of the tooth must first be understood. The tooth is a perfect device evolved through eons in biology, varying in different architectures in many species, adapted for the most optimal function. Much of the properties that contribute to the function of the tooth come from its hierarchical structure. The enamel is composed of 92 vol% hydroxyapatite, 2 vol.% collagen and 6 vol.% water. Dentin is a composite composed of 50 vol% mineral, collagen, and other proteins (~30 vol.%) and water (~20 vol.%)[45]. The enamel consists of a collection of nanorods of about 5 μm in diameter, each of which are bundles of hydroxyapatite nanocrystals 50 nm in diameter. This structure is a factor of enamel's hardness and toughness. Dentin is composed of tubules of about 1.5 μm in diameter that are perpendicular to the pulp[46]. The purpose of these tubules is for nutrient supply from the pulp to the dentin tissue[47]. The most important component of the tooth structure that is often overlooked is the cementum. It is made up of 50 vol% inorganic material (hydroxyapatite) and 50% organic material (water, collagen, proteoglycan)[48]. Since the cementum layer is at the interface between the dentin and the periodontal ligament, it is crucial that the cementum layer should be restored to prevent periodontal tissue attachment loss and create a healthy periodontium with healthy gingiva.

Previous studies suggest that enamel is made up of anisotropic hydroxyapatite nanorods[49]. There is a consequence to this assumption, as it proposes that enamel experiences fracturing frequently. It turns out that this is found not to be true. Studies support that enamel is measured to be about three times tougher than geological hydroxyapatite. This concludes that even though enamel is a

composite ceramic that is thought of as being brittle, the hydroxyapatite crystals have a unique and complex three-dimensional orientation within the structure of the enamel. Enamel also contains biological precipitates such as proteins and other inorganics that give rise to the sole properties and functionality of enamel[49,50].

The structural integrity of the tooth is primarily due to the interface between the dentin and enamel (the dentin-enamel junction (DEJ)) and that between the dentin and cementum, the (dentin-cementum junction (DCJ))[51]. From the dentin to the enamel or cementum, the mineral concentration increases in a gradient, allowing for structural integration between the dentin and the outer hard tissues of the tooth. An investigation studying nano-hardness and elastic modulus of human incisor teeth across the DEJ showed there were decreasing trends in both hardness and elastic modulus across the DEJ zone profiling from enamel to dentin. The continuous variation in the ratios of relative amount of enamel and dentin influenced the nano-mechanical property profiles across the DEJ. This is crucial in describing the characteristics of the DEJ, and the structural and mechanical integration of the two tissues. Increasing the contact area across the interface between the two hard tissues will allow the stresses to dissipate, reducing interfacial stress concentrations at the DEJ, and therefore fostering effective load transfer from the hard (brittle) enamel to soft (tough) dentin[52].

1.4 GEMSEC's Biomimetic Solution

Previous research in the Genetically Engineered Materials Science and Engineering Center (GEMSEC) laboratory evaluated the biomimetic approach to treat dentin hypersensitivity through an amelogenin protein-derived peptide called sADP5 (shortened human amelogenin-derived peptide 5) (**Figure 2)**[44].

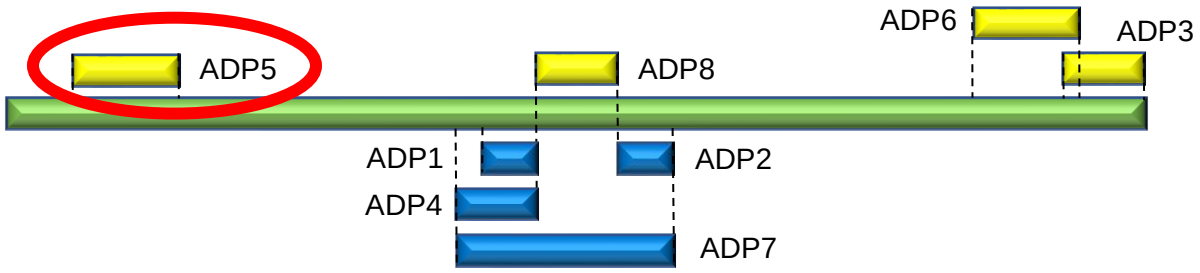

Figure 2: From the natural tooth forming protein, amelogenin (green), and the use of bioinformatics, peptides were select based on binding strength, biomineralization activity, kinetics, and mineral formation type. Four weak binders (yellow) and four strong binders (blue) were derived from amelogenin. For the purposes of creating a dental product, ADP5 was selected to be the most useful, as it replicated the kinetics of amelogenin[37].

In this study, it was proven that the sADP5 peptide exerted the fastest mineralization kinetics, close to that of amelogenin (the naturally occurring tooth developing protein)[26,53]. The remineralization of human enamel and restoration of dentin via formation of crystalline hydroxyapatite on artificially created white spot lesions with the introduction of Ca^{2+} and PO_4^{3-} ions under variable conditions was demonstrated. A major finding from this previous work suggested that the sADP5 can also deliver and incorporate fluoride ions into the remineralized layer even at low fluoride concentrations. After demonstrating the *in vivo* efficacy of peptide-guided remineralization treatment of demineralized hard tissues, a therapeutic dental product was proposed in the form of a lozenge to translate peptide-guided remineralization into clinical settings, and the first working prototype was developed (**Figure 3)**[54].

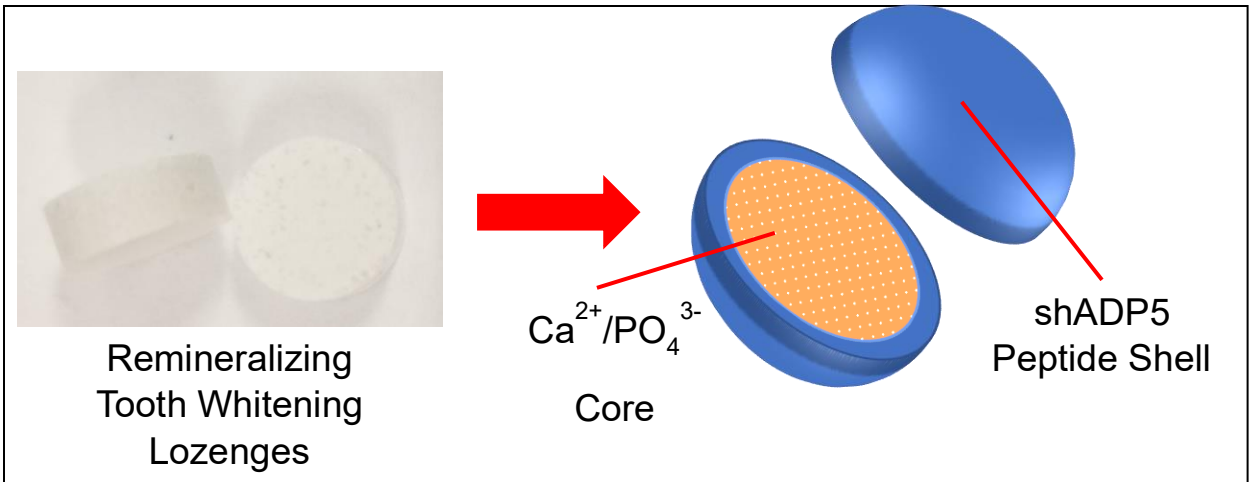

Figure 3: First working prototype of core-and-shell remineralizing tooth whitening lozenges

1.5 Remineralizing Tooth Whitening Lozenges

With the introduction of at-home whitening, and easy access to whitening methods prescribed by dental professionals, the popularity of dental whitening has increased significantly, allowing people to seek frequent whitening treatments[55]. The current whitening products contain abrasive chemicals or whiten through methods that can be damaging to the oral environment. These products include corrosive whitening agents such as hydrogen peroxide.

Over the counter (OTC) whitening strips and clinical whitening gels can contain peroxide-based chemicals at concentrations between 10% - 40%[56]. These chemicals dissolve the tooth mineral, making the enamel (the crown of the tooth) thinner. Although this gives a fresh and pristine surface, it is at the expense of the enamel by removing minerals on the surface.

The American Dental Association reports that enamel erosion caused by peroxide demineralization can lead to adverse effects: hypersensitivity (occurring in 64% of patients), gum recession, pulp inflammation and cavities due to regular use of whitening products[57–59].

It is proposed that the developed remineralizing and tooth whitening lozenge provides a healthier solution to teeth whitening without permanently damaging the mineral tissues. This is the ideal approach because the lozenges whiten the teeth by adding fresh mineral onto the surface, giving a whiter appearance while restoring the enamel[54]. This is made possible using amelogenin-derived peptides[26]. The lozenges may be used as a vehicle to deliver the active ingredients, which include Ca^{2+}, PO_4^{3-}, and the sADP5 peptide in a systematic way to biomimetically provide tooth whitening.

2. The Goals of this Thesis

The goal of this thesis is to analyze the effects of changing experimental conditions on mineral formation in response to precursor ions in solution. The hypothesis is that by changing experimental conditions such as pH, differences in mineral formation occurs. Previous observations explain what would happen when mixing $CaCl_2$ (a calcium source) with KH_2PO_4 (a phosphate source) in a biological buffer at a neutral pH of around 7.0. Hydroxyapatite mineral is formed through two pathways: homogeneous nucleation and heterogeneous nucleation[60]. Homogeneous nucleation occurs in solution, whereas heterogeneous nucleation occurs on a surface of foreign particles (**Figure 4)**[61].

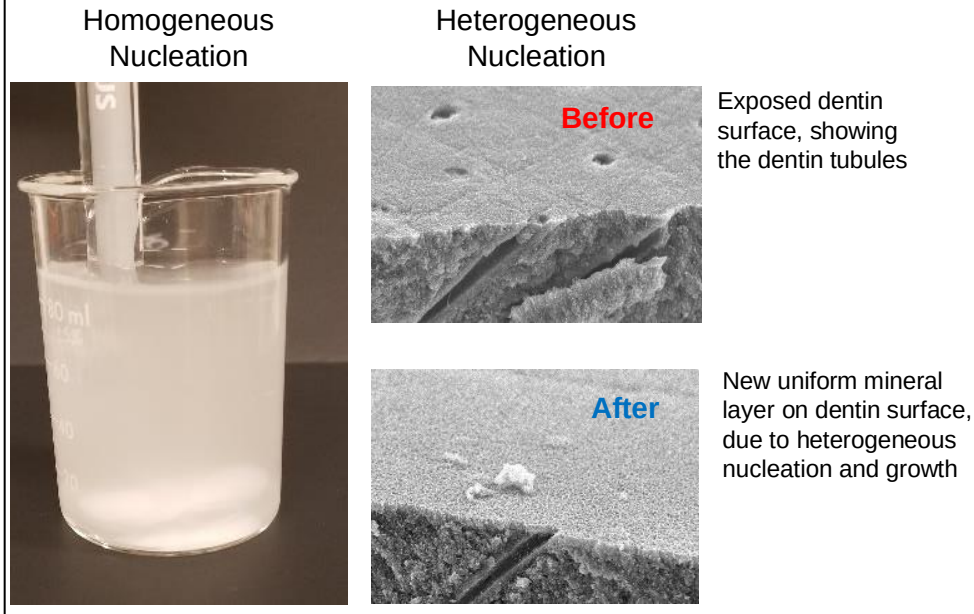

Figure 4: Physical illustrations of the homogeneous and heterogeneous nucleation of hydroxyapatite nanocrystals

Heterogenous nucleation is thermodynamically more favorable[62]. Theoretically, when homogeneous nucleation occurs, the formation of a solid nucleus leads to a Gibbs free energy change, given by the following formula[63]:

$$\Delta G = G_2 - G_1 = -V_S(G_v^L - G_v^S) + A^{SL}\gamma^{SL}$$

where V_S is the volume of a solid spherical nucleus, A^{SL} is the solid/liquid interface area, γ^{SL} is the solid/liquid interfacial energy, and $\Delta G_v = G_v^L - G_v^S$ is the difference between free energies per unit volume of the solid and liquid phases. At constant standard temperature and pressure, the thermodynamic definition of the volumetric Gibbs free energy is:

$$\Delta G_v = \Delta H_v - T\Delta S_v$$

where ΔH_v is the volumetric enthalpy change in the system, T is the temperature in the system, and ΔS_v is the volumetric entropic change in the system. Assuming a spherical nucleus, the simplified Gibbs free energy is written as:

$$\Delta G_r = G_2 - G_1 = -\frac{4}{3}\pi r^3(G_v^L - G_v^S) + 4\pi r^2\gamma^{SL}$$

During the process of nucleation, the radius of the nucleus reaches a critical radius before crystal growth occurs. The critical nucleus size is given by the following relation:

$$r^* = \frac{2\gamma^{SL}}{\Delta G_v}$$

The Gibbs free energy change that is involved in the radius growth of the nucleus to the critical size is the critical Gibbs free energy change of nucleation, or growth activation energy, given by:

$$\Delta G^* = \frac{16\pi(\gamma^{SL})^3}{3(\Delta G_v)^2}$$

Heterogeneous nucleation is energetically more preferred. It forms at preferential sites such as phase boundaries or nucleation site, solid surfaces, or foreign particles. At these sites, the effective surface energy is lower, and this diminishes the free energy barrier, facilitating

nucleation. The energetics for heterogeneous nucleation is like that of homogeneous nucleation, except for some additional characteristics. There are two additional interfacial energy terms that contribute to heterogeneous nucleation; the interfacial energy between the liquid and surface ($\gamma^{LS\prime}$) and the interfacial energy between the solid nucleus and the surface ($\gamma^{SS\prime}$). The interfacial energy balance in the plane of the surface gives the relation:

$$\gamma^{LS\prime} = \gamma^{SS\prime} + \gamma^{SL}\cos(\theta)$$

where θ is the wetting angle. Thus, the Gibbs free energy change for heterogeneous nucleation is as follows:

$$\Delta G_r^{het} = -V_S \Delta G_v + A^{SL}\gamma^{SL} + A^{SS'}\gamma^{SS'} - A^{SS'}\gamma^{LS\prime}$$

By utilizing the interfacial energy balance given above, this simplifies to:

$$\Delta G_r^{hom} F(\theta)$$

where, $F(\theta) = \frac{(2+\cos(\theta))(1-\cos(\theta))^2}{4}$. The critical nucleus size for heterogeneous nucleation is the same as homogeneous nucleation, however the critical Gibbs free energy change of nucleation is given by:

$$\Delta G_{het}^* = F(\theta)\Delta G_{hom}^*$$

Figure 5 below plots the energetic profile with particle radius growth.

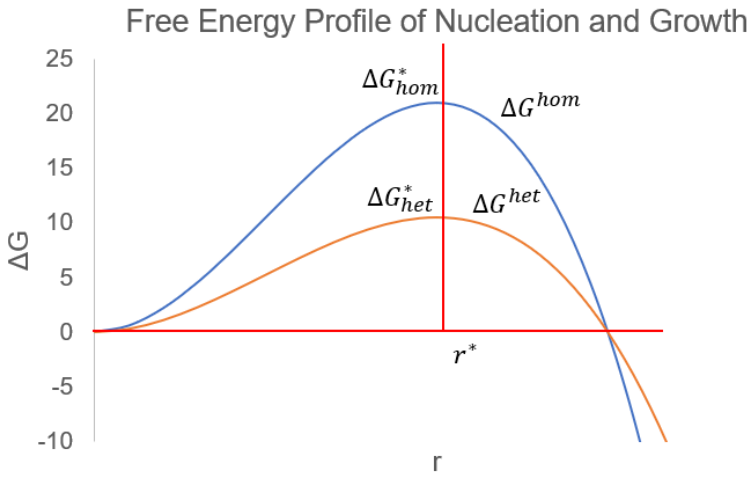

Figure 5: Free energy profile of nucleation and growth.

The biomineralization of inorganic materials involves the reaction of precursor reactants to produce nanoparticles of a desired biomaterial in an aqueous environment. The saturation of these particles in the system initiates nucleation. Due to the nucleation energy barrier, energy must be added to the system to overcome this energy barrier. This is mainly done by increasing the temperature of the system. In a biological environment, the temperature is constant, and thus the energy is obtained elsewhere. The source of this energy comes from the Gibbs free energy change in the mineralization reaction due to the chemical potentials of the molecules in the system, as well as the peptide involved as an enzymatic catalyst.

Energy that can be absorbed or released due to a change of the particle number of a given species is referred to as the chemical potential, and is defined as the partial Gibbs free energy as shown below:

$$\mu_i = \left(\frac{\partial G}{\partial N_i}\right)_{T,P,N_{j\neq i}}$$

Rearranging, this can be rewritten as $dG = \sum_{i=1}^{n} \mu_i dN_i$. This energy change is partly responsible for overcoming the nucleation energy barrier.

The sADP5 peptide functions as an enzymatic biocatalyst in the biomineralization of hydroxyapatite on the dentin surface. It increases the rate of the mineralization reaction at standard temperatures and pressures without being consumed in it by lowering the activation energy. The peptides lower the activation energy by bringing reactants closer and orienting them in a specific way or weakening their bonds[64]. It is hypothesized that the surface-bonded peptides serve as nucleation sites, and thus decrease the nucleation energy barrier.

The peptides work best within a narrow range of temperatures and pH called the optimal temperature and optimal pH. These have significant effects on the behavior of the enzyme. Therefore, optimizing these parameters against the enzymatic characteristics will allow for the development of specific crystallization methods. Since the saliva temperature is mostly constant, it is more significant to investigate the effects of pH on peptide function. If crystals are grown in a narrow pH range, then it is reasonable to assume that the crystals at the upper and lower limits will be fundamentally different. The pH is one of the most powerful ways to induce crystallization. Studies have shown that many proteins have been crystalized in the absence of precipitation just by manipulating the pH [65,66]. Due to this, relevant experiments have shown that the specific buffer must also be considered to be a potentially consequential variable [67–69]. The pH is a strong determination of the protonation state of each amino acid on a protein, and thus influences its electrostatic field, conformation, and how it interacts with other molecules. Considering the information described above, and the fact that nucleation is preferred to occur specifically on a tooth surface, heterogenous nucleation must be maximized, and homogenous nucleation minimized. The way to control this is by varying the pH[65,67–71].

The pH expresses the acidity or alkalinity of a solution and is dependent upon the concentration of free H^+ and OH^- in the solution. The governing chemical reaction to form hydroxyapatite is as follows[72–75]:

$$5CaCl_2 + 3KH_2PO_4 \xrightarrow{OH^-} Ca_5(PO_4)_3OH$$

Provided that the Ca^{2+} and PO_4^{3-} sources are supplied stoichiometrically, the hydroxyapatite formation will be limited by the concentration of free OH^- in the solution. A higher concentration of free OH^-, and thus a higher pH, will result in a higher rate of reaction. This can cause instant homogeneous nucleation, and not allow enough nucleation to occur on the surface[76–78]. But if the free OH^- concentration becomes too low, resulting in a low pH, the solution or environment becomes more acidic and can demineralize the hydroxyapatite mineral[79–82]. Which is why there should be some common middle ground, where heterogeneous nucleation can be fully maximized. By varying the pH of remineralization, observable effects in nucleation are to be expected. However, there are limitations to modeling the oral environment *in vitro*. The pH is adjusted easily *in vitro*, whereas the pH is dynamic and always fluctuating *in vivo*[83,84].
Saliva naturally prevents demineralization by neutralizing the acid produced by the oral bacteria[85–87]. It can enhance remineralization by supplying calcium, phosphate, and fluoride to enamel and dentin[88]. It is shown that an equilibrium between demineralization and remineralization exists in the dental biofilm. With increased metabolic activity of the bacterial, the oral pH decreases and is then restored to the resting pH by the buffering effect of the saliva[85,86,89]. If the resting saliva pH and buffering capacity are low, the saliva is more acidic, so for patients with low saliva secretion, buffering capacity, or resting pH, they are more likely to

experience demineralization of tooth minerals and form caries[90–94]. The critical pH for the enamel and dentin below which demineralization occurs has been reported to be in the range of 5.2–5.8 and 6.0–6.9, respectively[16,95–100]. Saliva has a normal pH range of 6.2 – 7.6 with 6.7 being the average pH[101,102]. This thesis explored the upper normal pH range between 6.7 and 7.4 to show that minor changes in pH even at the normal range can have significant effects in mineralization.

The objective was to utilize the previously identified sADP5 peptide to create a mineral layer on the exposed dentin surface for the purpose of preventing and treating dentin hypersensitivity[44]. The effects of pH on biomineralization were observed using Scanning Electron Microscopy (SEM). The fundamental experimental approach was to prepare dentin disk samples about 1-4 mm thick, completely expose the dentin surface, biomineralize the sample in solution given specified pH values and precursor ion concentration levels, then characterize the mineral formation and thickness through SEM. Through SEM, it was shown that heterogeneous nucleation occurred in a narrow pH range, and therefore an optimal pH value was determined. The newfound knowledge was implemented in the remineralizing and whitening lozenge previously formulated in the laboratory to act as a delivery system for the remineralizing active ingredients, where further production and testing was carried out, and the dissolution and remineralization of these lozenges were characterized by calcium assays and SEM characterization respectively. This implementation was to justify that the pH experiments and the results can translate to a dental product formulation. **Figure 6** shows a schematic of the general mechanism of action for the remineralization approach.

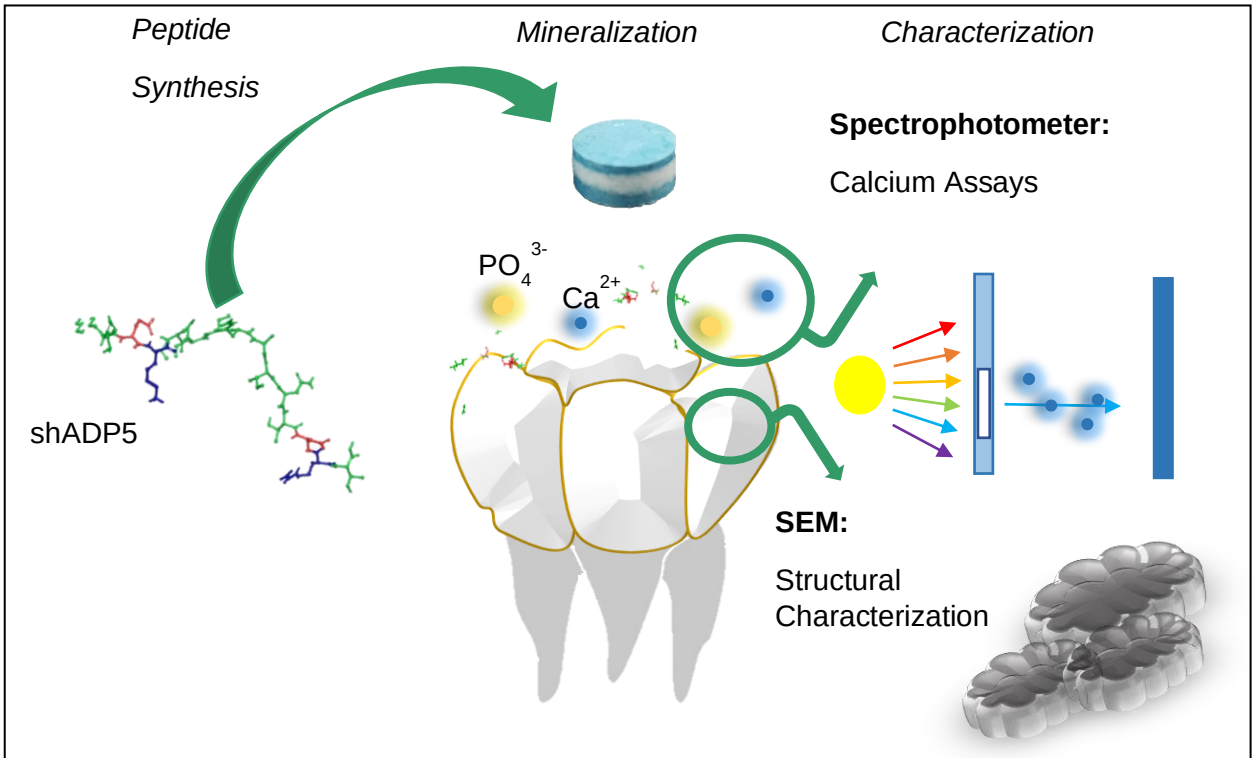

Figure 6: Mechanism of action for remineralization approach

3. Materials and Methods

3.1 pH Effect on Nucleation and Growth

3.1.1 Sample Preparation

Extracted human molar teeth with no restorations were collected from the UW Dental School and disinfected in 10% aqueous bleach solutions. Prior to the experiments, the teeth were cleaned to remove visible blood, gross debris, and soft connective tissue using a dental scaler under a light microscope. Samples chosen for testing were taken for cutting. The samples were cut into discs of about 1-4 mm thick using a low speed saw (IsoMet™, Buehler, Lake Bluff, IL, United States), as illustrated in **Figure 7**.

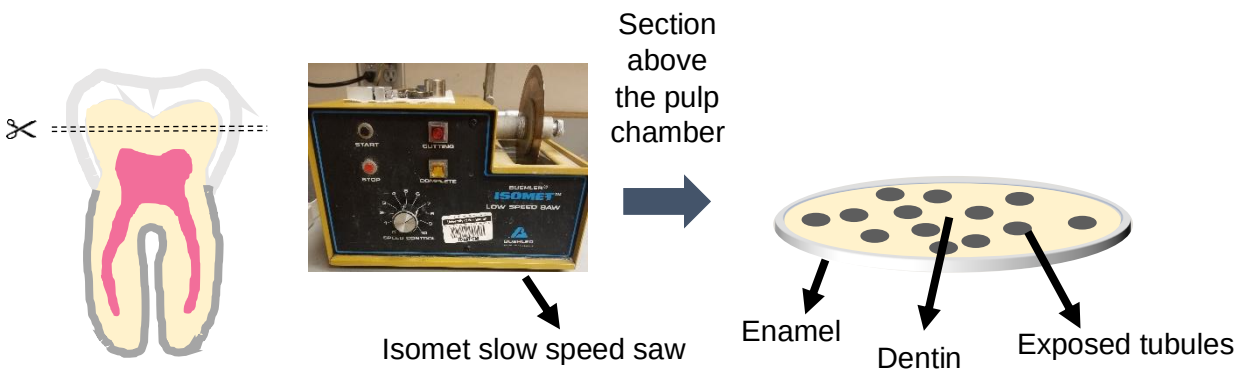

Figure 7: Dentin discs are cut using an IsoMet™ slow speed saw, then polished and etched to expose the dentin surface.

The discs were sonicated to remove any deposited debris from cutting and kept submerged in DI water to avoid the tooth samples from drying out. The samples were polished using diamond lapping films to a 0.1 µm finish. The dentin surfaces were demineralized with 35% phosphoric acid gel for 10 seconds, then rinsed with DI water to remove the excess acid etchants from the surface. The samples were then divided into control and test groups (**Table 1**).

Table 1: Test groups and treatment procedures

Test Groups	Treatment Procedure	pH	Trials
Group 1 (Negative Control)	No Treatment	NA	3
Group 2	0.8 mM Peptide, 10 min 4.8 mM Ca^{2+} / 2.88 mM PO_4^{3-}	6.7 ± 0.02	3
Group 3	0.8 mM Peptide, 10 min 4.8 mM Ca^{2+} / 2.88 mM PO_4^{3-}	6.8 ± 0.02	3
Group 4	0.8 mM Peptide, 10 min 4.8 mM Ca^{2+} / 2.88 mM PO_4^{3-}	6.9 ± 0.02	3
Group 5	0.8 mM Peptide, 10 min 4.8 mM Ca^{2+} / 2.88 mM PO_4^{3-}	7.0 ± 0.02	3
Group 6	0.8 mM Peptide, 10 min 4.8 mM Ca^{2+} / 2.88 mM PO_4^{3-}	7.3 ± 0.02	3
Group 7	0.8 mM Peptide, 10 min 4.8 mM Ca^{2+} / 2.88 mM PO_4^{3-}	7.4 ± 0.02	3

3.1.2 Peptide Design and Synthesis[54]

The sADP5 peptide was designed and synthesized using a protocol developed and optimized by the peptide synthesis team, supervised by Dr. Deniz Yucesoy, in the GEMSEC group[26,44,54]. The molecular characteristics of this peptide is reported in **Table 2**.

Table 2: Molecular characteristics of the sADP5 peptide.

shADP5 AA Sequence	MW	pI	G.R.A.V.Y.	Charge
SYEKSHSQAINTDRT	1736.8	6.47	-1.627	0

An automated solid-phase synthesizer (CS336X; CS-Bio, Menlo Park, CA, USA) was used to synthesize the peptide through Fmoc-chemistry. The Wang resin (Novabiochem, West Chester, PA, USA) was mixed with 20% piperidine in dimethylformamide (DMF; Sigma-Aldrich, St. Louis, MO, USA) to remove the Fmoc group. The entering amino acid, which was side-chain protected, was activated with N,N,N′,N′-Tetramethyl-O-(1H-benzotriazol-1- yl)uronium hexafluorophosphate (HBTU; Sigma-Aldrich, St Louis, MO, USA) in DMF, then transported into the synthesizer and incubated with the Wang resin for a duration of 45 minutes. The resin was washed away with DMF, and the same protocol was applied for the addition of each of the incoming amino acids. The overall synthesis reaction was monitored by UV-absorbance at 301 nm. The resulting resin-bound peptides following synthesis were cleaved and the side-chain was de-protected using reagent-K [TFA/thioanisole/H2O/phenol/ ethanedithiol (87.5:5:5:2.5), Sigma-Aldrich, St Louis, MO, USA]. The peptides were solidified using a cold ether solution, and the crude peptides were purified by RP-HPLC with up to >98% purity (Gemini 10u C18 110A column). The peptide sequence was verified by MALDI-TOF mass spectrometry with a reflectron (RETOF-MS) on an Autoflex II (Bruker Daltonics, Billerica, MA, USA).

3.1.3 Solution Remineralization Procedure

Before being treated, the previously cut samples were hydrated and equilibrated in 50 mM HEPES buffer for 2 hours at a pH of 7.4. The lyophilized sADP5 peptide was dissolved in 50 mM HEPES buffer to a final concentration of 0.8 mM. The specimens were submerged under the sADP5 solution for 10 min at 37^{o}C in an incubator. Control specimens were identically prepared only by submerging in buffer alone. At the end of 10 min, the samples were rinsed twice with deionized water.

Solutions of 9.6 mM $CaCl_2$ and 5.6 mM KH_2PO_4 were prepared in 50 mM HEPES buffer. The solutions were aliquoted and adjusted to pH's of 6.7, 6.8, 6.9, 7.0, 7.3, and 7.4. The control and peptide-coated samples were placed in 1.5 mL of Ca^{2+} and an equal volume of PO_4^{3-} was added to achieve a final concentration of 4.8 mM of Ca^{2+} and 2.88 mM of PO_4^{3-}. This was done for each of the various pH conditions. The specimens were left in a shaker for 2 hours at room temperature (**Figure 8**), then removed and rinsed with DI water. The specimens were then dried out in a desiccator to get rid of any humidity on the sample in preparation for SEM characterization. **Figure 9** shows a schematic of the biomineralization mechanism.

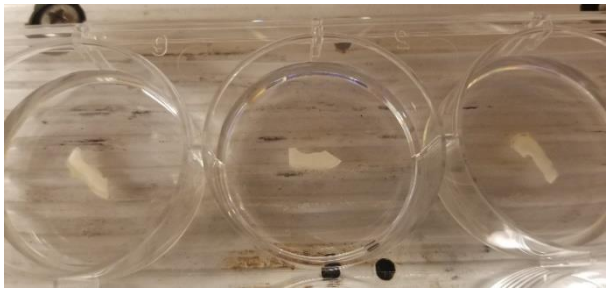

Figure 8: Dentin specimens in a 6-well plate on an automated shaker. From left to right, the well plates contain the specimens in the remineralization solution at pH's of 6.8, 7.0, and 7.4 respectively.

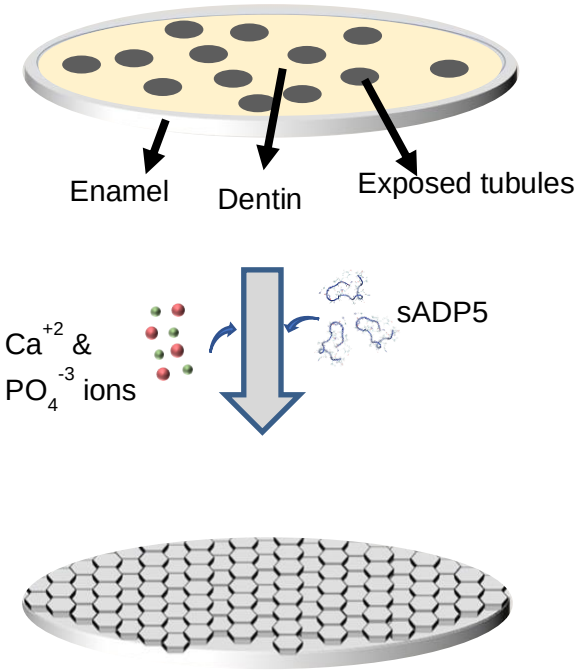

Figure 9: Schematic of biomineralization mechanism.

3.1.4 SEM Characterization – Imaging

After remineralization was completed, a scanning electron microscope (SEM) was used to characterize surface texture and morphology. This allows the thickness of the newly formed mineral layer in the applicable cross sections to be observed. Before remineralization, notches were made at the back of each specimens. After the remineralization step was completed, the

specimens were carefully fractured into two segments. The pieces were mounted on a SEM stub with the mineralized surface facing up and angled to observe the cross-section. The samples were again placed in vacuum to remove residual moisture. Prior to imaging, the samples were sputter coated with 5 nm of gold (SPI-Sputter Module Coater, SPI Supplies, West Chester, PA, United States). The SEM microscope used was a JEOL-JSM-6010 microscope, operating at 10 kV.

3.2 Remineralizing Tooth Whitening Lozenge Production and Testing at Optimal pH

3.2.1 Materials[54]

Reagent purchases: 99% $CaCl_2$ from Alfa Aesar (Ward Hill, MA); KH_2PO_4 from USB Corporation (Cleveland, OH); 99% D-Sorbitol from Sigma-Aldrich (Milwaukee, WI); all other chemicals and reagents were purchased from Sigma-Aldrich (Milwaukee, WI), and used as received unless otherwise noted. Equipment and facilities: tooth samples were donated from the UW School of Dentistry; a Minolta ChromaMeter CR-200 was obtained from Glen H. Johnson, DDS, MS, UW School of Dentistry; a ball mill, 9 mm metal dies, and a Carver Model 3853 hydraulic press were used with the courtesy of the UW Department of Materials Science & Engineering.

3.2.2. Lozenge Formulation and Fabrication

Using the base formulation developed by Dr. Deniz Yucesoy and Dr. Hanson Fong in the GEMSEC group, lozenges were designed and structured in a bilayer architecture, as shown in **Figure 10** and **Figure 11.**

Figure 10: Single image of layered lozenge

Figure 11: Multi-colored lozenges with layered architecture

The outer, colored layers contain the active remineralizing peptide sADP5, and the inner white layer contains the ionic Ca^{2+} and PO_4^{3-} sources. Other inactive ingredients, such as sorbitol (sweetener), magnesium stearate (lubricant), mint/peppermint (flavoring), and food dye (color) are also included in the formulation. **Table 3** lists the ingredients and measurements for the formulation.

Table 3: Formula of layered remineralizing tooth whitening lozenges.

	Peptide Layer Formula		Core Layer Formula	
Ingredients	**Amount (mg)**	**Weight %**	**Amount (mg)**	**Weight %**
Peptide	3	3	N/A	N/A
$CaCl_2H_2O$	N/A	N/A	94	55
KH_2PO_4	N/A	N/A	56	33
Mg-Stearate	1	1	1.7	1
Sorbitol	10	10	17	10
Peppermint	4	4	1.7	1
Talc	82	82	N/A	N/A
Total	100	100	170	100

To allow for homogeneous dissolution, the blend was prepared using the weight percentages shown in Table 3. The blend was grounded in a ball mill at 87 rpm for 20 hours into a fine

powder before being put under direct uniaxial compression for fabrication. The lozenges were compressed at a force of 11,000 lbf **Figure 12**.

Figure 12: Carver tablet press (left) and a schematic of 9 mm tablet punch press die (right)

3.2.3 Lozenge Dissolution and Remineralization

To successfully analyze lozenge dissolution and remineralization, the oral environment must be simulated as accurately as possible. A USP Dissolution 2 Apparatus is commonly used, in which the artificial saliva is stirred with a paddle and shaft system at room temperature and at 100 rpm. The apparatus setup used for dissolution and remineralization is illustrated below in **Figure 13.**

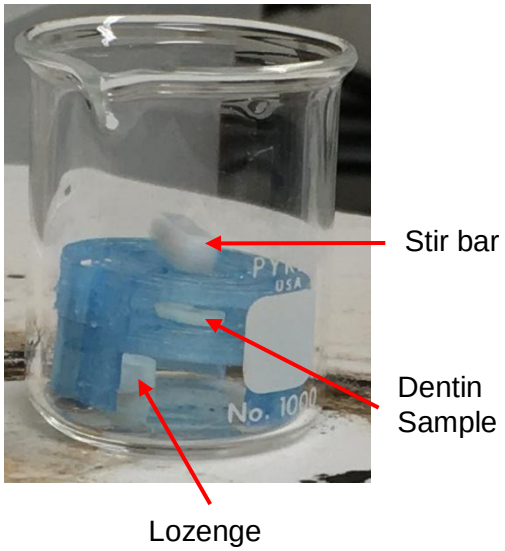

Figure 13: Setup of apparatus

The tooth samples were prepared the same way described in section 3.1.1 and were placed in the system with the lozenge. 10 mL of artificial saliva at the optimal pH determined by the pH experiments, later shown to be 6.8, was placed into the system at the start. 5 mL of saliva was removed and replaced every minute to simulate swallowing and secretion of fresh saliva. The full dissolution and remineralization processes were done in 15 minutes. Samples analyzed were treated with 1 round, 2 rounds, and 3 rounds of treatment to track mineral thickness growth. The tooth samples were then drip rinsed for 30 seconds with DI water to remove any residual lozenge debris that might be deposited on the tooth surface. The samples were transported to a vacuumed desiccator to dry the samples before performing SEM characterization.

3.2.4 Calcium Assay

A calcium assay is carried out to analyze the calcium consumption during remineralization. During lozenge dissolution and remineralization, 50 µL samples of the saliva were taken at different moments and placed in 1.5 mL Eppendorf vials. The saliva was sampled at the start (t =

0 minutes), then at t = 5 minutes, then at t = 10 minutes, then finally at t = 15 minutes. A QuantiChrom™ Calcium Assay Kit was used to carry out the analysis. 5 μL samples were taken from each of the time-point samples and pipetted in a 96-well plate along the same row. A 1:1 volume ratio of reagent A and reagent B from the calcium assay kit were mixed to prepare the dye. 200 μL of the dye is mixed with each of the 5 μL samples, as followed by the protocol in the kit. The well plate is directly placed in a Tecan Safire™ spectrophotometer to measure the optical density of the saliva samples. A linear correlation between the optical density and calcium concentration is used to determine the calcium consumption over time.

3.2.5 SEM Characterization – Imaging

Before remineralization, notches were made at the back of each specimens. After the remineralization step was completed, the specimens were carefully fractured into two segments. The pieces were mounted on a SEM stub with the mineralized surface facing up and angled to observe the cross-section. The samples were again placed in vacuum to remove residual moisture. Prior to imaging, the samples were sputter coated with 5 nm of gold (SPI-Sputter Module Coater, SPI Supplies, West Chester, PA, United States). The SEM microscope used was a JEOL-JSM-6010 microscope, operating at 10 kV.

3.2.6 Statistical Analysis – Hypothesis Testing

To describe data discrepancies, a hypothesis test is performed using a t-test approach. Given that the null hypothesis is $H_0: \bar{x} = \mu$, where $\bar{x}$ is the sample mean and μ is the population mean, and the significance level is chosen to be $\alpha = 0.05$, the t-value is calculated by the following relationship:

$$t = \frac{(\bar{x} - \mu)}{\sigma\sqrt{N}}$$

where σ is the sample standard deviation and N is the sample size. The relevant statistical values are reported in **Table 5** below for each time point shown in **Figure 15** in the results, given a sample size of $N = 3$**.**

4. Results

4.1 pH Effects on Nucleation and Growth

The first set of results are that from the pH experiments (**Figure 14)**. The control sample that was compared is shown in Figure 13a. Notice the exposed tubules on the dentin surface. Figure 13b shows the first mineralized test at a pH of 6.7. Figures 5c, d, e, f, and g are the results for pH's 6.7, 6.8, 6.9, 7.0, 7.3, and 7.4 respectively.

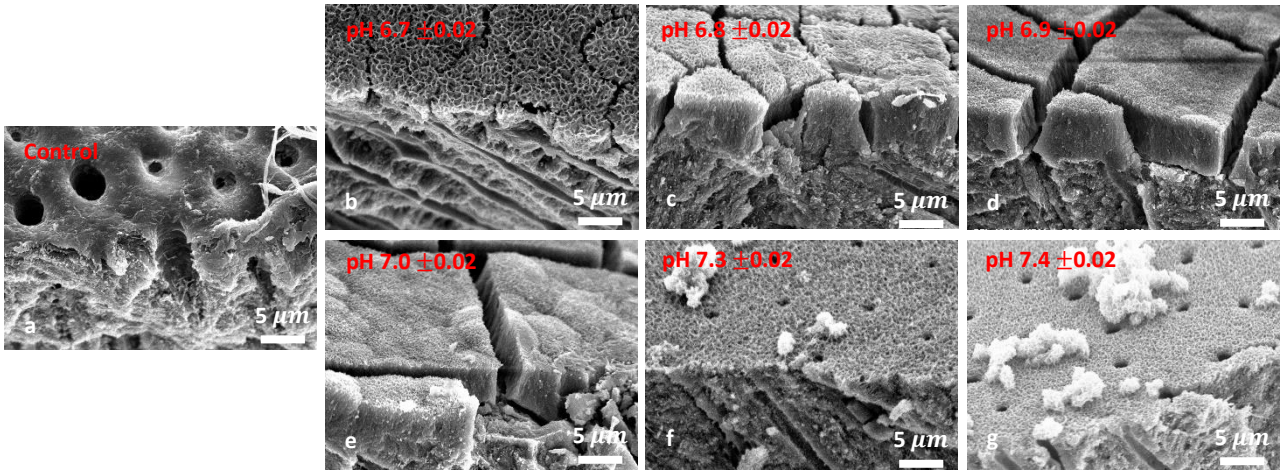

Figure 14: a. No peptide control sample; b. Mineralization at pH 6.7; c. pH 6.8; d. pH 6.9; e. pH 7.0; f. pH 7.3; g. pH 7.4

4.2 Remineralizing Tooth Whitening Lozenge Production and Testing at Optimal pH

The calcium assay results are illustrated in **Figure 15**, showing the free calcium concentration in the saliva throughout time. **Table 4** below **Figure 15** shows the dissolution results of each trial run after one round of lozenge remineralization.

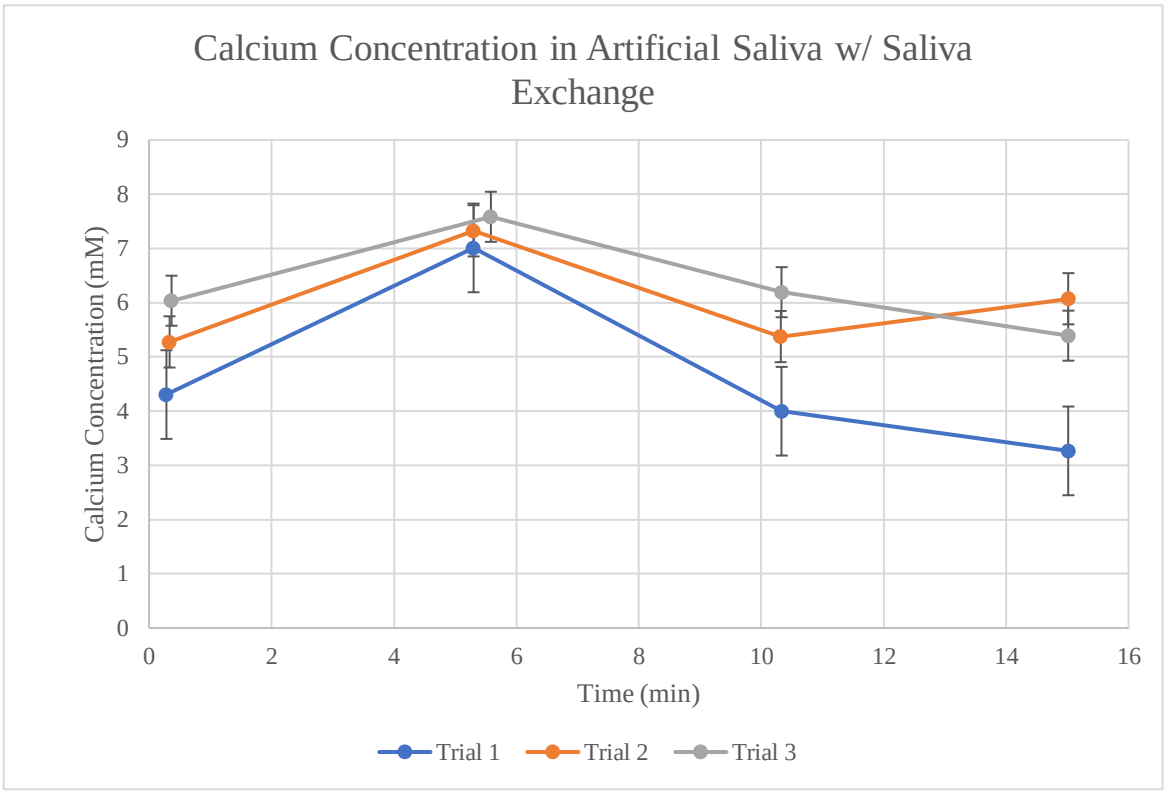

Figure 15: Calcium concentration in saliva at a pH of 6.8 throughout time

Table 4: Lozenge dissolution results

Trial	Amount Disintegrated (mg)	Dissolution Rate (mg/min)
1	130	8.67
2	150	10.00
3	130	8.67
Average	137	9.17
Stdev	±9.57	±0.64

The plots suggest that there is an increase in calcium concentration as time progresses, followed by a steady decrease. This is due to the lozenge dissolving quickly at the start, and when the disintegration rate slows down, the reaction consumes calcium for hydroxyapatite formation, decreasing the calcium concentration. The resulting dissolution measurements reported in Table 4 suggest that about 70% of the lozenge is dissolved in 15 minutes.

Figure 16 shows the SEM images of 1, 2, and 3 rounds of lozenge remineralization under a controlled pH of 6.8.

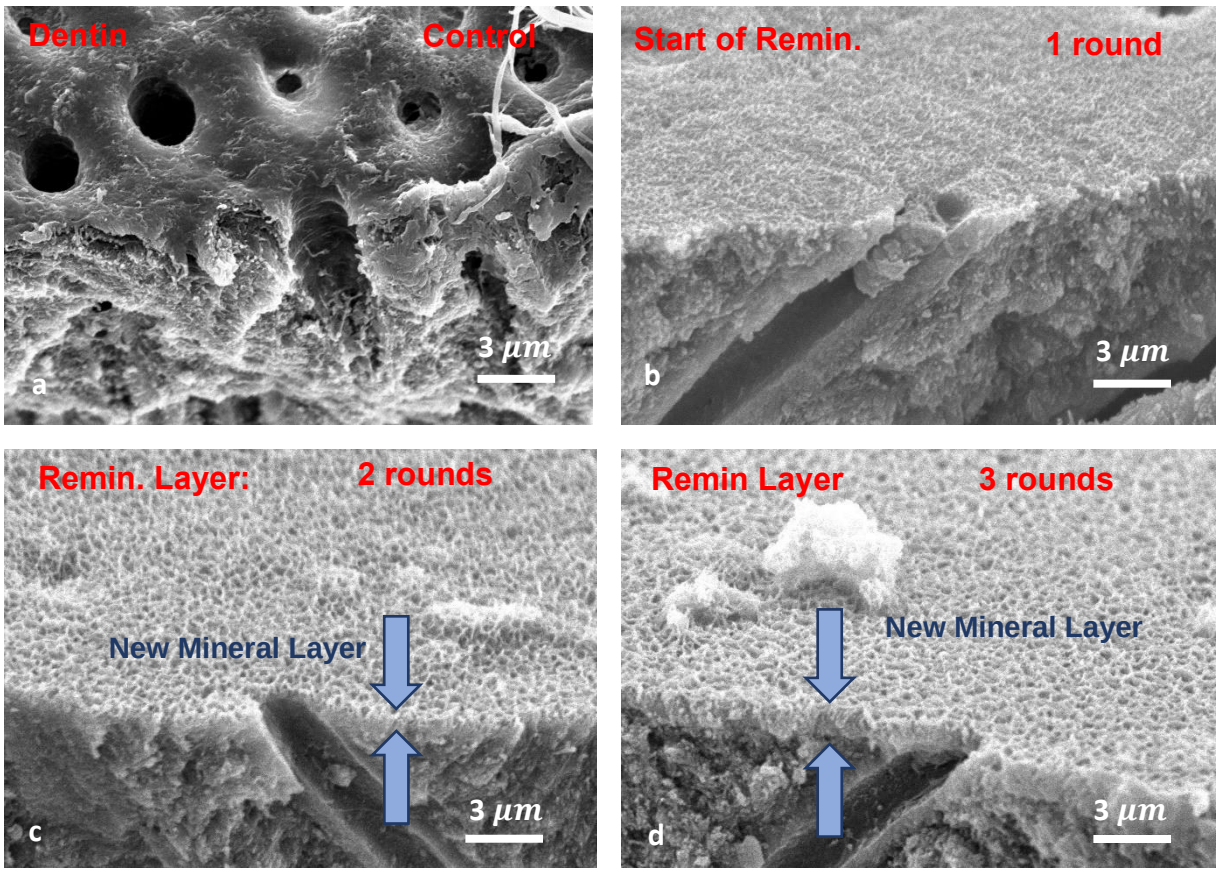

Figure 16: SEM images of layer by layer remineralization of exposed dentin: (a) control sample (b)1 round, (c) 2 rounds, and (d) 3 rounds of lozenge remineralization in saliva at a pH of 6.8

The images clearly depict the increasing mineral thickness with each new application of the lozenges.

Table 5 below summarizes the results of the calcium assay hypothesis t-test.

Table 5: Statistical parameters for t-test hypothesis testing

Time Point	Sample Mean ($\bar{x}$)	Population Mean (μ)	Sample Standard Deviation (σ)	t-value	p-value
0 minutes	5.2 mM	4.9 mM	0.87 mM	0.23	0.84
5 minutes	7.3 mM	6.7 mM	0.29 mM	1.3	0.32
10 minutes	5.2 mM	4.6 mM	1.1 mM	0.30	0.79
15 minutes	4.9 mM	3.7 mM	1.5 mM	0.47	0.68

5. Discussions

5.1 pH Effects on Nucleation and Growth

The impact from this experiment's results indicates that the pH has a significant effect on the thickness of mineral on the surface. Such small changes in pH can have a major effect on mineralization[103–105]. At a pH of 6.8, heterogeneous nucleation was more present than at the higher pH conditions of 7.3 and 7.4. However, this does not yet have any clinical significance, since the pH range is limited to the normal saliva pH. It is still observed that lowering the pH of mineralization to a certain range minimizes homogenous nucleation and maximizes the amount of mineral formed on the tooth.

To understand these phenomena, the pH effects on mineral formation and peptide-ion interaction must be discussed. Being reminded of the governing equilibrium ionic reaction given below:

$$5Ca^{2+} + 3PO_4^{3-} + OH^- \overset{HEPES}{\longleftrightarrow} Ca_5(PO_4)_3OH$$

If the pH of the system is increased, and therefore the OH^- concentration is increased, the reaction is forward driven, increasing the rate of reaction. The opposite is true when the pH is decreased. This explains mineralization at higher pH levels, whether it is homogeneous or heterogeneous nucleation and growth, and demineralization at lower pH levels. Provided that the system becomes saturated with hydroxyapatite molecules, heterogeneous nucleation is most likely to occur, starting at an onset pH. As the pH increases in value, both homogeneous and heterogeneous nucleation can occur together. This explains the effects shown in the SEM results, where mineral formation on the surface was less prevalent at the higher pH conditions of 7.3 and 7.4.

The pH of the system also contributes to the behavior and function of the sADP5 peptide introduced to the process. Shown in the peptide sequence, the peptide contains amino acids that provide multiple protonation and deprotonation sites (**Figure 17)**[44,54].

S Y E K S H S Q A I N T D R T

Figure 17: sADP5 peptide sequence with color coded protonation/deprotonation amino acid domains. Neutrally charged (green); positively charged (blue); negatively charged (red).

These sites are represented by the color-coded amino acid symbols in **Figure 17,** where the neutrally charged amino acids are coded in green, positively charged (Lysine and Arginine) in blue, and negatively charged (Glutamic acid and Aspatic acid) in red at the physiological pH of 7.0. These are determined based on the pKa value estimates of each amino acid and their protonation or deprotonation sites. One amino acid that is considered an exception is histidine. Lone histidine is known to be positively charged at a physiological pH of 7.0. However, when it is linked to other amino acids by peptide bonds, the only hydrogen bonding site is exposed by the histidine side chain. At pH values above 6, the histidine side chain becomes negatively charged due to the side chain having a pKa value of 6. Another important characteristic of the peptide is its isoelectric point (pI). The pI is the estimated pH value in which the peptide has a net zero charge. At pH values above the pI, the net charge of the peptide is negative; at pH values below the pI, the net charge of the peptide is positive (**Figure 18).**

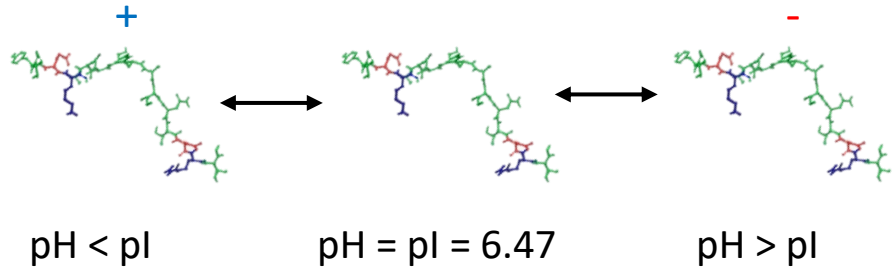

Figure 18: Schematic of peptide charge at pH value above and below the pI value

Using the Prot pi protein tool, a pI value of the sADP5 peptide is estimated to be 6.47 (https://www.protpi.ch/Calculator/ProteinTool). From titration data predictions performed by the center of biochemistry and bioanalytics at the Zurich University of Applied Sciences, the charge of the peptide at the determined optimal pH of 6.8 is calculated to be -0.3 coulombs. This slight negative charge would improve the peptide-ion interaction with the positively charged calcium ions in the system, recruiting the ions to the dentin surface, and catalyzing the mineralization of hydroxyapatite. The proposed mechanism of action is that the positively charged domains in the peptide attach to the negatively charged dentin surface, whereas the negatively charged domains recruit the positively charged calcium ions. However, this mechanism is limited to a specific pH range, because the charges of each amino acid is subjected to change if it falls out of that pH range. Not only does the peptide interact with the surrounding ions in the environment, but it also interacts with itself, resulting in a specific conformation and therefore its function.

Due to that the density of the mineral is high, during the SEM sample preparation, the mineral cracks. At a pH of 6.8, a preferred mineral thickness of 3-5 μm is obtained after just one round remineralization. On the other hand, high pH enables a continuous remineralized layer that occludes the tubules, but it is thinner and less dense. Ideally, full occlusion of the tubules is desired, along with thick and dense mineral formation with minimal cracking. The next steps of this experiment are to do multiple rounds of mineralization, utilizing the effects of the experimental conditions that were observed. One example is to first mineralize a tooth sample at a high enough pH to allow for occlusion of tubules, then mineralize at a pH such as 6.8 to increase the thickness of the mineral. This way, the tubules can be occluded and obtain mineral formation of desirable thickness. To fully complete the pH experiments, pH values below the

normal range should also be tested to observe remineralization under a saliva condition where the tooth mineral is subjected to demineralization.

5.2 Remineralizing Tooth Whitening Lozenge Production and Testing at Optimal pH

A biomimetic remineralizing lozenge was developed to restore and whiten the tooth through a peptide-guided remineralization approach. The lozenge was made to deliver the remineralizing agents required in a systematic way for effective remineralization. To ensure this sequential delivery, the lozenges were structured in a bilayer architecture. The outer layers contain the active sADP5 peptide, and the inner layer contains the calcium and phosphate ions. The remainder inactive ingredients were determined by researching the ingredients on the most common lozenges, and mints on the market. Sorbitol, magnesium stearate, peppermint flavoring, and talc were used for sweeting, lubrication, flavoring, and filling material respectively. A hydraulic press was used to fabricate the lozenges at a compression force of 11,000 lbf. Artificial saliva was prepared, and the lozenges were dissolved for 15 minutes and tested for remineralization with the dentin samples previously prepared. A calcium assay and SEM microscopy were carried out to analyze calcium consumption and structural characterization. The calcium assays signified the calcium consumption of the mineralization reaction over time. **Figure 15** above shows a sample experiment that had nine repetitions. The error bars on each point represent the population standard deviation among all repeated experiments. As observed in the plot, there seems to be a discrepancy in the concentration readings at each time point. These are due to limitations in lozenge manufacturing, time sampling, and calcium assay preparation. The lozenges are not all identically the same, so the dissolution behavior may also be different. Though this may only cause minor error. Most of the error comes from the time sampling. Small volumes of the saliva are sampled out, and even smaller volumes are used for

calcium assays. To verify that these discrepancies are statistically insignificant, a hypothesis test was performed. The results of the hypothesis t-test suggest that the measurement discrepancies introduced above are statistically insignificant, because the p-values at each time point is significantly larger than a significance level of 0.05. Therefore, we accept the null hypothesis that $\bar{x} = \mu$ with 95% confidence.

As shown in the SEM images in **Figure 16**, After 3 rounds of lozenge application at a pH of 6.8, the mineral thickness is estimated to be about 1.5 μm. A continuous mineral layer of plate-like hydroxyapatite nanocrystals form on the dentin surface, indicating effective remineralization by the lozenge. Multiple repetitions of these experiments showed similar behaviors of dentin remineralization. The low yield of mineral thickness after 3 rounds of treatment is due to the limitations of the delivery method. The calcium and phosphate sources supplied to the modeled oral environment is limited by what is in the lozenge. In addition, each treatment round is limited to the lozenge lifetime of 15 minutes during dissolution.

5.3 Study Comparison and Limitations

Hydroxyapatite crystal growth has been studied for as long as 50 years. One of the first methods of studying the growth kinetics of hydroxyapatite was done by seeding stable supersaturated calcium phosphate solutions with crystals at room temperature and at constant physiological pH conditions, as studied by G.H Nancollas and M.S Mohan at the State University of New York at Buffalo in 1970[106]. Before then, there was a major difficulty in understanding how the stoichiometry of the precipitated hydroxyapatite nanoparticles had always been less than the required calcium to phosphate molar ratio of 1.67. This led to the production of other calcium phosphate phase derivatives as a result including dicalcium phosphate, tricalcium phosphate, and octacalcium phosphate at physiological pH conditions between 6.3 to 7.5[107–111]. The technique of

seeded growth produced highly reproducible results for the formation of hydroxyapatite, allowing for further studies to be performed over a range of pH conditions. The results suggested an appreciable increase in the crystallization rate of hydroxyapatite with an increased pH going from 7.4 to 7.8 in increments of 0.2. It was also mentioned that at pH levels above 7.8, there was spontaneous precipitation of calcium phosphate, limiting heterogeneous nucleation and crystal growth. Utilizing the sADP5 peptide-guided remineralization approach, just hydroxyapatite crystals are formed on the dentin surface by simply introducing the calcium and phosphate precursor ions at a 1.67 calcium to phosphate molar ratio at room temperature and a constant physiological pH range, without the need for crystal seeding. An increase in the crystallization rate was also observed between pH values of 6.7 to 7.0, above which spontaneous precipitation of calcium phosphate occurred. The study done by Nancollas and Mohan described above suggested that this spontaneous precipitation should have occurred at pH levels above 7.8. Due to the peptide's function as a biological catalyst, it is proposed that the peptide increases the crystallization rate even further, lowering the free energy barrier required for the spontaneous precipitation of calcium phosphate, and thus occurs at a lower pH level than 7.8.

As hydroxyapatite synthesis techniques became more advanced, hydrothermal methods using elevated temperatures and pressures in an aqueous environment allowed for the synthesis of hydroxyapatite with a specific crystal shape[112]. Researchers have studied the influence of pH on the crystallization of hydroxyapatite, synthesized by hydrothermal methods at comparatively low temperatures, and have concluded that the pH value is a significant parameter variable in manipulating crystal morphology[113,114]. However, the temperatures ranged between 60 ℃ and 140 ℃, which is still not ideal in an oral environment, and would denature biological proteins or peptides, depriving them of their functions. Fortunately, the peptide-guided remineralization

approach is done at room temperature and does not have the limitations of hydrothermal methods.

Although this work avoided some of the limitations described above, it has some of its own. Many steps are required for the synthesis methods for peptide-guided hydroxyapatite crystallization, especially in the peptide design and synthesis. To mass produce these peptides would be relatively expensive and time consuming. High-throughput automated techniques would need to be developed to optimize this approach. Additionally, the teeth samples prepared for remineralization can differ slightly in size, but this difference in minimized as much as possible for each test group. The in-solution remineralization procedure is completed in a modeled environment that is in ideal conditions (room temperature and a constant pH). The oral environment is dynamic and saliva pH can vary, going as low as a pH level of 2. The pH range selected for the pH experiments were within the normal pH range, so the results do not completely describe clinical significance, but pH ranges outside the normal limit will be explored in the future. The justification for this was to first explore the effects of minor pH changes on the nucleation and growth of hydroxyapatite crystal using a peptide-guided remineralization approach, which was not yet studied before.

6. Conclusions

6.1 pH Effects on Nucleation and Growth

This study successfully shows that there are significant changes in mineralization when subjected to pH changes or changes in precursor concentrations regarding its effects specifically on the kinetics of hydroxyapatite crystallization and peptide-ion interactions. With this, it was shown that the type of nucleation, heterogeneous (desired) or homogeneous (undesired), can be controlled with pH. The results of the pH experiments were limited to a specific pH range between 6.7 to 7.4, which was chosen to explore the pH effects even under the smallest changes at the normal saliva pH range. Heterogeneous nucleation was more prevalent at a pH range between 6.7 and 7.0, with the optimal pH observed to be at 6.8. It was explained that this phenomenon was due to the effect that pH had on the nucleation kinetics of hydroxyapatite crystallization. Furthermore, the sADP5 peptide works best at a specific pH called the optimal pH. To verify that this is consistent with the observed optimal pH level of 6.8, an enzyme activity titration versus pH will be performed in future experiments. It was also demonstrated that the new mineral formation physically integrates to the structure of the dentin surface, mimicking the interface of the dentin-enamel junction or dentin-cementum junction. This is significant because all the current approaches for dental restorations today fail to achieve this structural integrity.

6.2 Remineralizing Tooth Whitening Lozenge Production and Testing at Optimal pH

A bilayer lozenge was developed for efficient delivery of the remineralizing components using a peptide-guided remineralization approach. From the pH experiments, the optimal pH of remineralization was determined to be 6.8. This is comparable to the average human saliva pH of 6.7. This is expected, as the experiments were only limited to the normal saliva pH range.

However, the oral environment is also subjected to sudden changes in pH. This may damage the peptide, depleting it of its function. Thus, pH cycling experiments will be performed in the future. The lozenge remineralization process was done at a controlled pH of 6.8. It was repeatedly shown that each round of lozenge treatment at this pH added new mineral to the surface and thickened the mineral layer by layer. The lozenges, and their potential for success have inspired many other dental products such as toothpastes, mouthwashes, gels, varnishes, etc. The lozenges were not only shown to restore the enamel or dentin, but also provide a whitening effect, making this a therapeutic and cosmetic dental product.

7. Future Work

The foundation of this thesis has provided insight to future work that can further support developing pH effect hypotheses. Now that the upper pH range of 6.7-7.4 has been explored, it is just as important to investigate the lower range between 6.2 and 6.7, as well as under demineralizing conditions below a pH level of 5.5. These experiments would justify whether future formulations will work under dynamic pH conditions in the oral environment. Final conclusions cannot yet be made on the probability of one nucleation type (heterogeneous or homogeneous nucleation) over another. To fully understand this, light transmission profiles must be completed in the case of homogeneous versus heterogeneous hydroxyapatite formation with the aid of a spectrophotometer. To verify the crystal structure obtained from the new hydroxyapatite mineral layer, an X-ray diffraction (XRD) analysis will be performed. Mechanical durability tests will be done to test the durability if the new mineral layer. Titration experiments measuring peptide charge versus pH will need to be replicated based on similar methods performed by the Center for Biochemistry and Bioanalytics at the Zurich University of Applied Sciences assess the electrochemical behavior of the peptide. This will need to be followed by molecular dynamics simulations to justify the conformational behavior of the peptide on the surface of dentin. Following the lozenge remineralization tests, the whitening effects will be quantified using a high-performance camera specifically set up at a custom photo-taking station equipped with LED lighting and diffuser, then performing a color analysis by analyzing the images using ImageJ and Adobe Lightroom color analysis software. The objectives for future work also include third party validated clinical trials and discussing marketing strategies for the lozenges with our partners at Proctor and Gamble. Furthermore, the motivation

behind this thesis, and the protocols developed can easily be translated to propose many more dental products.

8. Impact on the Future Development of New Formulations

The work described has provided insight in the development of new therapeutic and cosmetic dental formulations. Methods for the research and development of dental products such as mouthwashes, gels, varnishes, or even chewing gum can be performed similarly to what is depicted in the guide above for the new toothpaste design. These products would be the first of its kind to provide a healthy and additive approach for tooth whitening and restoration. Not only will this impact the future of dental products, but it will change every day dental care and the oral health care industry.

The pH experiments have allowed for the control of a new process parameter. As was shown, slight changes in the pH change how thick the new mineral layer forms over time. Since every consumer that would use a given product would have a different saliva pH, it is crucial that the proper usage instructions are translated regarding the frequency and duration of application. The goal is to provide a net gain of new mineral to the oral environment until all the demineralized enamel is restored back, then to permanently prevent any demineralization in the future. This requires collaboration with dental health professionals, so that the correct information is provided to their patients. With the results and knowledge acquired from the lozenge tests, dentists and their patients will now have a convenient solution to enamel demineralization associated dental conditions.

9. References

1. Waters, N. E. Biomechanics in clinical dentistry. *J. Dent.* (1989) doi:10.1016/0300-5712(89)90021-3.

2. Shashvatt, U., Aris, H. & Blaney, L. Evaluation of Animal Manure Composition for Protection of Sensitive Water Supplies Through Nutrient Recovery Processes. in *Chemistry and Water: The Science Behind Sustaining the World's Most Crucial Resource* (2017). doi:10.1016/B978-0-12-809330-6.00013-1.

3. Teh, S. J. & Lai, C. W. Carbon nanotubes for dental implants. in *Applications of Nanocomposite Materials in Dentistry* (2018). doi:10.1016/B978-0-12-813742-0.00005-5.

4. Miglani, S., Aggarwal, V. & Ahuja, B. Dentin hypersensitivity: Recent trends in management. *J. Conserv. Dent.* **13**, 218 (2010).

5. Bartold, P. M. Dentinal hypersensitivity: A review. *Australian Dental Journal* (2006) doi:10.1111/j.1834-7819.2006.tb00431.x.

6. Dental Health Foundation. Dental Caries (Tooth Decay). *Dent. Heal. Found. Irel.* (2015).

7. Petersson, L. G. The role of fluoride in the preventive management of dentin hypersensitivity and root caries. *Clinical Oral Investigations* (2013) doi:10.1007/s00784-012-0916-9.

8. Kuroiwa, M., Kodaka, T., Kuroiwa, M. & Abe, M. Dentin Hypersensitivity. Occlusion of Dentinal Tubules by Brushing With and Without an Abrasive Dentifrice. *J. Periodontol.* (1994) doi:10.1902/jop.1994.65.4.291.

9. Markowitz, K. A new treatment alternative for sensitive teeth: A desensitizing oral rinse. *J. Dent.* (2013) doi:10.1016/j.jdent.2012.09.007.

10. Cheng, X. *et al.* Comparative effect of a stannous fluoride toothpaste and a sodium fluoride toothpaste on a multispecies biofilm. *Arch. Oral Biol.* (2017) doi:10.1016/j.archoralbio.2016.10.030.

11. Sharif, M. O., Iram, S. & Brunton, P. A. Effectiveness of arginine-containing toothpastes in treating dentine hypersensitivity: A systematic review. *Journal of Dentistry* (2013) doi:10.1016/j.jdent.2013.01.009.

12. Hines, D. *et al.* Effect of a stannous fluoride toothpaste on dentinal hypersensitivity: In vitro and clinical evaluation. *J. Am. Dent. Assoc.* (2019) doi:10.1016/j.adaj.2019.01.006.

13. Yang, Z. Y., Wang, F., Lu, K., Li, Y. H. & Zhou, Z. Arginine-containing desensitizing toothpaste for the treatment of dentin hypersensitivity: A meta-analysis. *Clin. Cosmet. Investig. Dent.* (2016) doi:10.2147/CCIDE.S95660.

14. Aguiar, J. D., Medeiros, I. S., e Souza Junior, M. H. S. & Loretto, S. C. Influence of the extended use of desensitizing toothpastes on dentin bonding, microhardness and roughness. *Braz. Dent. J.* (2017) doi:10.1590/0103-6440201601292.

15. Blinkhorn, A. & Mekertichian, K. Fluoride and dental health. in *Handbook of Pediatric Dentistry: Fourth Edition* (2013). doi:10.1016/B978-0-7234-3695-9.00005-5.

16. Neel, E. A. A. *et al.* Demineralization–remineralization dynamics in teeth and bone. *International Journal of Nanomedicine* (2016) doi:10.2147/IJN.S107624.

17. Bosshardt, D. D. Biological mediators and periodontal regeneration: A review of enamel matrix proteins at the cellular and molecular levels. in *Journal of Clinical Periodontology* (2008). doi:10.1111/j.1600-051X.2008.01264.x.

18. Margolis, H. C., Beniash, E. & Fowler, C. E. Role of macromolecular assembly of enamel matrix proteins in enamel formation. *Journal of Dental Research* (2006) doi:10.1177/154405910608500902.

19. Bègue-Kirn, C., Krebsbach, P. H., Bartlett, J. D. & Butler, W. T. Dentin sialoprotein, dentin phosphoprotein, enamelysin and ameloblastin: Tooth-specific molecules that are distinctively expressed during murine dental differentiation. *Eur. J. Oral Sci.* (1998) doi:10.1046/j.0909-8836.1998.eos106510.x.

20. Nanci, A. *et al.* Comparative immunochemical analyses of the developmental expression and distribution of ameloblastin and amelogenin in rat incisors. *J. Histochem. Cytochem.* (1998) doi:10.1177/002215549804600806.

21. Fong, C. D., Černý, R., Hammarström, L. & Slaby, I. Sequential expression of an amelin gene in mesenchymal and epithelial cells during odontogenesis in rats. *Eur. J. Oral Sci.* (1998) doi:10.1111/j.1600-0722.1998.tb02193.x.

22. MacDougall, M. *et al.* Cloning, characterization and immunolocalization of human ameloblastin. *Eur. J. Oral Sci.* (2000) doi:10.1034/j.1600-0722.2000.108004303.x.

23. Oida, S. *et al.* Amelogenin gene expression in porcine odontoblasts. *J. Dent. Res.* (2002) doi:10.1177/154405910208100204.

24. Papagerakis, P. *et al.* Expression of amelogenin in odontoblasts. *Bone* (2003) doi:10.1016/S8756-3282(02)00978-X.

25. Le, T. Q., Zhang, Y., Li, W. & Denbesten, R. K. The effect of LRAP on enamel organ epithelial cell differentiation. *J. Dent. Res.* (2007) doi:10.1177/154405910708601114.

26. M., G. *et al.* Cementomimetics-constructing a cementum-like biomineralized microlayer via amelogenin-derived peptides. *International journal of oral science* (2012).

27. Goldberg, H. A., Warner, K. J., Li, M. C. & Hunter, G. K. Binding of bone sialoprotein, osteopontin and synthetic polypeptides to hydroxyapatite. *Connect. Tissue Res.* (2001) doi:10.3109/03008200109014246.

28. Gu, L. S. *et al.* Immobilization of a phosphonated analog of matrix phosphoproteins within cross-linked collagen as a templating mechanism for biomimetic mineralization. *Acta Biomater.* (2011) doi:10.1016/j.actbio.2010.07.036.

29. Kim, J. *et al.* Functional biomimetic analogs help remineralize apatite-depleted demineralized resin-infiltrated dentin via a bottom-up approach. *Acta Biomater.* (2010) doi:10.1016/j.actbio.2009.12.052.

30. Capriotti, L. A., Beebe, T. P. & Schneider, J. P. Hydroxyapatite surface-induced peptide folding. *J. Am. Chem. Soc.* (2007) doi:10.1021/ja070356b.

31. Taller, A., Grohe, B., Rogers, K. A., Goldberg, H. A. & Hunter, G. K. Specific adsorption of osteopontin and synthetic polypeptides to calcium oxalate monohydrate crystals. *Biophys. J.* (2007) doi:10.1529/biophysj.106.101881.

32. Wazen, R. M. *et al.* In vivo functional analysis of polyglutamic acid domains in recombinant bone sialoprotein. *J. Histochem. Cytochem.* (2007) doi:10.1369/jhc.6A7046.2006.

33. Zhang, S., Gangal, G. & Uludağ, H. 'Magic bullets' for bone diseases: Progress in rational design of bone-seeking medicinal agents. *Chemical Society Reviews* (2007) doi:10.1039/b512310k.

34. Tye, C. E. *et al.* Delineation of the hydroxyapatite-nucleating domains of bone sialoprotein. *J. Biol. Chem.* (2003) doi:10.1074/jbc.M211915200.

35. Pampena, D. A. *et al.* Inhibition of hydroxyapatite formation by osteopontin phosphopeptides. *Biochem. J.* (2004) doi:10.1042/BJ20031150.

36. Fan, Y., Sun, Z. & Moradian-Oldak, J. Controlled remineralization of enamel in the presence of amelogenin and fluoride. *Biomaterials* (2009) doi:10.1016/j.biomaterials.2008.10.019.

37. Ruan, Q., Zhang, Y., Yang, X., Nutt, S. & Moradian-Oldak, J. An amelogenin-chitosan matrix promotes assembly of an enamel-like layer with a dense interface. *Acta Biomater.* (2013) doi:10.1016/j.actbio.2013.04.004.

38. Shafiei, F. *et al.* Leucine-rich amelogenin peptide (LRAP) as a surface primer for biomimetic remineralization of superficial enamel defects: An in vitro study. *Scanning* (2015) doi:10.1002/sca.21196.

39. Kirkham, J. *et al.* Self-assembling peptide scaffolds promote enamel remineralization. *J. Dent. Res.* (2007) doi:10.1177/154405910708600507.

40. Li, Q. L. *et al.* A novel self-assembled oligopeptide amphiphile for biomimetic mineralization of enamel. *BMC Biotechnol.* (2014) doi:10.1186/1472-6750-14-32.

41. Wu, D. *et al.* Hydroxyapatite-anchored dendrimer for in situ remineralization of human tooth enamel. *Biomaterials* (2013) doi:10.1016/j.biomaterials.2013.03.053.

42. Fowler, C. E., Li, M., Mann, S. & Margolis, H. C. Influence of surfactant assembly on the formation of calcium phosphate materials - A model for dental enamel formation. *J. Mater. Chem.* (2005) doi:10.1039/b503312h.

43. Gungormus, M. *et al.* Self assembled bi-functional peptide hydrogels with biomineralization-directing peptides. *Biomaterials* (2010) doi:10.1016/j.biomaterials.2010.06.010.

44. Dogan, S. *et al.* Biomimetic Tooth Repair: Amelogenin-Derived Peptide Enables in Vitro Remineralization of Human Enamel. *ACS Biomater. Sci. Eng.* (2018) doi:10.1021/acsbiomaterials.7b00959.

45. Purk, J. H. Morphologic and structural analysis of material-tissue interfaces relevant to dental reconstruction. in *Material-Tissue Interfacial Phenomena: Contributions from Dental and Craniofacial Reconstructions* (2017). doi:10.1016/B978-0-08-100330-5.00008-X.

46. Arendsa, J., Stokroos, I., Jongebloed, W. G. & Ruben, J. The diameter of dentinal tubules in human coronal dentine after demineralization and air drying: A combined light microscopy and sem study. *Caries Res.* (1995) doi:10.1159/000262052.

47. Ghannam, M. G. & Bordoni, B. *Anatomy, Head and Neck, Pulp (Tooth)*. *StatPearls* (2019).

48. Ho, S. P. *et al.* Structure, chemical composition and mechanical properties of human and rat cementum and its interface with root dentin. *Acta Biomater.* (2009) doi:10.1016/j.actbio.2008.08.013.

49. White, S. N. *et al.* Biological organization of hydroxyapatite crystallites into a fibrous continuum toughens and controls anisotropy in human enamel. *J. Dent. Res.* (2001) doi:10.1177/00220345010800010501.

50. Bechtle, S., Habelitz, S., Klocke, A., Fett, T. & Schneider, G. A. The fracture behaviour of dental enamel. *Biomaterials* (2010) doi:10.1016/j.biomaterials.2009.09.050.

51. Hand, A. R. & Frank, M. E. *Fundamentals of Oral Histology and Physiology*. *John Wiley & Sons, Inc.* (2014).

52. Fong, H., Sarikaya, M., White, S. N. & Snead, M. L. Nano-mechanical properties profiles across dentin-enamel junction of human incisor teeth. *Mater. Sci. Eng. C* (1999) doi:10.1016/s0928-4931(99)00133-2.

53. Gungormus, M. *et al.* Regulation of in vitro calcium phosphate mineralization by combinatorially selected hydroxyapatite-binding peptides. *Biomacromolecules* (2008) doi:10.1021/bm701037x.

54. Yucesoy, D. T. Peptide-Guided Dental Tissue Regeneration for Oral Care. *ProQuest Dissertations and Theses* (2018).

55. Perdigão, J. Dental whitening--revisiting the myths. *Northwest Dent.* (2010).

56. Carey, C. M. Tooth whitening: What we now know. *J. Evid. Based. Dent. Pract.* (2014) doi:10.1016/j.jebdp.2014.02.006.

57. Joiner, A. The bleaching of teeth: A review of the literature. *Journal of Dentistry* (2006) doi:10.1016/j.jdent.2006.02.002.

58. Tredwin, C. J., Naik, S., Lewis, N. J. & Scully Cbe, C. Hydrogen peroxide tooth-whitening (bleaching) products: Review of adverse effects and safety issues. *British Dental Journal* (2006) doi:10.1038/sj.bdj.4813423.

59. Hanks, C. T., Fat, J. C., Corcoran, J. F. & Wataha, J. C. Cytotoxicity and Dentin Permeability of Carbamide Peroxide and Hydrogen Peroxide Vital Bleaching Materials, in vitro. *J. Dent. Res.* (1993) doi:10.1177/00220345930720051501.

60. Fang, W. *et al.* Hydroxyapatite Crystal Formation in the Presence of Polysaccharide. *Cryst. Growth Des.* (2016) doi:10.1021/acs.cgd.5b01235.

61. Oxtoby, D. W. Homogeneous nucleation: Theory and experiment. *J. Phys. Condens. Matter* (1992) doi:10.1088/0953-8984/4/38/001.

62. Zeng, Q. & Xu, S. Thermodynamics and Characteristics of Heterogeneous Nucleation on Fractal Surfaces. *J. Phys. Chem. C* (2015) doi:10.1021/acs.jpcc.5b07709.

63. Zhigilei, L. Nucleation and growth kinetics Nucleation and growth - the main mechanism of phase transformations in materials. *Cl. Lect.* (2010).

64. Edition, E. Enzymes and Energy. 4–6 (2003).

65. Glusker, J. P. Protein Crystallization. Techniques, Strategies, and Tips Edited by Terese M. Bergfors. International University Line, 1999. ISBN 0963681753. *Cryst. Growth Des.* (2003) doi:10.1021/cg020059c.

66. McPherson, A. & Cudney, B. Optimization of crystallization conditions for biological macromolecules. *Acta Crystallogr. Sect. FStructural Biol. Commun.* (2014) doi:10.1107/S2053230X14019670.

67. Collins, B., Stevens, R. C. & Page, R. Crystallization optimum solubility screening: Using crystallization results to identify the optimal buffer for protein crystal formation. *Acta Crystallogr. Sect. F Struct. Biol. Cryst. Commun.* (2005) doi:10.1107/S1744309105035244.

68. Izaac, A., Schall, C. A. & Mueser, T. C. Assessment of a preliminary solubility screen to improve crystallization trials: Uncoupling crystal condition searches. *Acta Crystallogr. Sect. D Biol. Crystallogr.* (2006) doi:10.1107/S0907444906018385.

69. Jancarik, J., Pufan, R., Hong, C., Kim, S. H. & Kim, R. Optimum solubility (OS) screening: An efficient method to optimize buffer conditions for homogeneity and crystallization of proteins. *Acta Crystallogr. Sect. D Biol. Crystallogr.* (2004) doi:10.1107/S0907444904010972.

70. McPherson, A. & Cudney, B. Optimization of crystallization conditions for biological macromolecules. *Acta Crystallogr. Sect. FStructural Biol. Commun.* **70**, 1445–1467 (2014).

71. Larson, S. B., Day, J. S., Glaser, S., Braslawsky, G. & McPherson, A. The structure of an antitumor CH2-domain-deleted humanized antibody. *J. Mol. Biol.* (2005) doi:10.1016/j.jmb.2005.03.036.

72. Brown, P. W. & Fulmer, M. Kinetics of Hydroxyapatite Formation at Low Temperature. *J. Am. Ceram. Soc.* (1991) doi:10.1111/j.1151-2916.1991.tb04324.x.

73. Fulmer, M. T. & Brown, P. W. Effects of Na2HPO4 and NaH2PO4 on hydroxyapatite formation. *J. Biomed. Mater. Res.* (1993) doi:10.1002/jbm.820270815.

74. TenHuisen, K. S. & Brown, P. W. Formation of calcium-deficient hydroxyapatite from α-tricalcium phosphate. *Biomaterials* (1998) doi:10.1016/S0142-9612(98)00131-8.

75. Francis, M. D. & Webb, N. C. Hydroxyapatite formation from a hydrated calcium monohydrogen phosphate precursor. *Calcif. Tissue Res.* (1970) doi:10.1007/BF02196214.

76. Turnbull, D. Kinetics of heterogeneous nucleation. *J. Chem. Phys.* (1950) doi:10.1063/1.1747588.

77. Lu, K. & Li, Y. Homogeneous Nucleation Catastrophe as a Kinetic Stability Limit for Superheated Crystal. *Phys. Rev. Lett.* (1998) doi:10.1103/PhysRevLett.80.4474.

78. Tobin, M. C. Theory of phase transition kinetics with growth site impingement. III. Mixed heterogeneous–homogeneous nucleation and nonintegral exponents of the time. *J. Polym. Sci. Polym. Phys. Ed.* (1977) doi:10.1002/pol.1977.180151217.

79. Sperber, G. H. & Buonocore, M. G. Effect of Different Acids on Character of Demineralization of Enamel Surfaces. *J. Dent. Res.* (1963) doi:10.1177/00220345630420022001.

80. Margolis, H. C., Zhang, Y. R., Lee, C. Y., Kent, R. L. & Moreno, E. C. Kinetics of enamel demineralization in vitro. *J. Dent. Res.* (1999) doi:10.1177/00220345990780070701.

81. Anderson, P. & Elliott, J. C. Subsurface Demineralization in Dental Enamel and Other Permeable Solids During Acid Dissolution. *J. Dent. Res.* (1992) doi:10.1177/00220345920710080301.

82. Grobler, S. R., Senekal, P. J. & Laubscher, J. A. In vitro demineralization of enamel by orange juice, apple juice, Pepsi Cola and Diet Pepsi Cola. *Clin. Prev. Dent.* (1990).

83. Hicks, J., Garcia-Godoy, F. & Flaitz, C. Biological factors in dental caries enamel structure and the caries process in the dynamic process of demineralization and remineralization (part 2). *J. Clin. Pediatr. Dent.* (2004) doi:10.17796/jcpd.28.2.617404w302446411.

84. Naumova, E. A. *et al.* Dynamic changes in saliva after acute mental stress. *Sci. Rep.* (2014) doi:10.1038/srep04884.

85. Kleinberg, I. & Jenkins, G. N. The pH of dental plaques in the different areas of the mouth before and after meals and their relationship to the pH and rate of flow of resting saliva. *Arch. Oral Biol.* (1964) doi:10.1016/0003-9969(64)90015-9.

86. Edgar, W. M. The role of saliva in the control of ph changes in human dental plaque. *Caries Res.* (1976) doi:10.1159/000260206.

87. Abelson, D. C. & Mandel, I. D. The Effect of Saliva on Plaque pH in vivo. *J. Dent. Res.* (1981) doi:10.1177/00220345810600090101.

88. Mavazesh, M. & Kumar, S. K. S. Measuring salivary flow: Challenges and opportunities. *Journal of the American Dental Association* (2008).

89. Dirks, O. B. Posteruptive Changes in Dental Enamel. *J. Dent. Res.* (1966) doi:10.1177/00220345660450031101.

90. Jensen, M. E. Responses of interproximal plaque pH to snack foods and effect of chewing sorbitol-containing gum. *J. Am. Dent. Assoc.* (1986) doi:10.14219/jada.archive.1986.0187.

91. Markovic, N., Abelson, D. C. & Mandel, I. D. Sorbitol Gum in Xerostomics: The Effects on Dental Plaque pH and Salivary Flow Rates. *Gerodontology* (1988) doi:10.1111/j.1741-2358.1988.tb00307.x.

92. Dodds, M. W. J., Hsieh, S. C. & Johnson, D. A. The Effect of Increased Mastication by Daily Gum-chewing on Salivary Gland Output and Dental Plaque Acidogenicity. *J. Dent. Res.* (1991) doi:10.1177/00220345910700120101.

93. Stephan, R. M. Changes in Hydrogen-Ion Concentration on Tooth Surfaces and in Carious Lesions. *J. Am. Dent. Assoc.* (1940) doi:10.14219/jada.archive.1940.0178.

94. Englander, H. R., Shklair, I. L. & Fosdick, L. S. The Effects of Saliva on the pH and Lactate Concentration in Dental Plaques:I. Caries-Rampant Individuals. *J. Dent. Res.* (1959) doi:10.1177/00220345590380051201.

95. Delgado, A. J. & Olafsson, V. G. Acidic oral moisturizers with pH below 6.7 may be harmful to teeth depending on formulation: A short report. *Clinical, Cosmetic and Investigational Dentistry* (2017) doi:10.2147/CCIDE.S140254.

96. Delgado, A. J., Olafsson, V. G. & Donovan, T. E. pH and Erosive Potential of Commonly Used Oral Moisturizers. *J. Prosthodont.* (2016) doi:10.1111/jopr.12324.

97. DePaola, D. P. Saliva: The precious body fluid. *Journal of the American Dental Association* (2008).

98. Surmont, P. A. & Martens, L. C. Root surface caries: an update. *Clinical preventive dentistry* (1989).

99. Hoppenbrouwers, P. M. M., Driessens, F. C. M. & Borggreven, J. M. P. M. The mineral solubility of human tooth roots. *Arch. Oral Biol.* (1987) doi:10.1016/0003-9969(87)90085-9.

100. Sung, Y.-H., Son, H.-H., Yi, K. & Chang, J. Elemental analysis of caries-affected root dentin and artificially demineralized dentin. *Restor. Dent. Endod.* (2016) doi:10.5395/rde.2016.41.4.255.

101. Larsen, M. J. & Pearce, E. I. F. Saturation of human saliva with respect to calcium salts. *Arch. Oral Biol.* (2003) doi:10.1016/S0003-9969(03)00007-4.

102. Baliga, S., Muglikar, S. & Kale, R. Salivary pH: A diagnostic biomarker. *J. Indian Soc. Periodontol.* (2013) doi:10.4103/0972-124X.118317.

103. Yu, L. & Ng, K. Glycine crystallization during spray drying: The pH effect on salt and polymorphic forms. *J. Pharm. Sci.* (2002) doi:10.1002/jps.10225.

104. Abbona, F., Lundager Madsen, H. E. & Boistelle, R. Crystallization of two magnesium phosphates, struvite and newberyite: Effect of pH and concentration. *J. Cryst. Growth* (1982) doi:10.1016/0022-0248(82)90242-1.

105. Reddy, M. M. & Wang, K. K. Crystallization of calcium carbonate in the presence of metal ions: I. Inhibition by magnesium ion at pH 8.8 and 25°C. *J. Cryst. Growth* (1980) doi:10.1016/0022-0248(80)90095-0.

106. Nancollas, G. H. & Mohan, M. S. The growth of hydroxyapatite crystals. *Arch. Oral Biol.* (1970) doi:10.1016/0003-9969(70)90037-3.

107. Francis, M. D. SOLUBILITY BEHAVIOR OF DENTAL ENAMEL AND OTHER CALCIUM PHOSPHATES. *Ann. N. Y. Acad. Sci.* (1965) doi:10.1111/j.1749-6632.1965.tb34834.x.

108. Boskey, A. L. & Posner, A. S. Conversion of amorphous calcium phosphate to microcrystalline hydroxyapatite. A pH-dependent, solution-mediated, solid-solid conversion. *J. Phys. Chem.* (1973) doi:10.1021/j100638a011.

109. Becke-Goehring, M. Phosphorus and its Compounds, Bd. 1: Chemistry, von J. R. Van Wazer. Interscience Publishers, New York-London 1958. 1. Aufl., XIII, 954 S., geb. $ 27.50. *Angew. Chemie* (1961) doi:10.1002/ange.19610731513.

110. Brown, W. E. Crystal growth of bone mineral. *Clin. Orthop. Relat. Res.* (1966) doi:10.1097/00003086-196600440-00021.

111. Brown, W. E., Lehr, J. R., Smith, J. P. & William Frazier, A. Crystallography of octacalcium phosphate [5]. *Journal of the American Chemical Society* (1957) doi:10.1021/ja01576a068.

112. Yoshimura, M., Suda, H., Okamoto, K. & Ioku, K. Hydrothermal synthesis of biocompatible whiskers. *J. Mater. Sci.* (1994) doi:10.1007/BF00352039.

113. Liu, J. *et al.* The influence of pH and temperature on the morphology of hydroxyapatite synthesized by hydrothermal method. *Ceram. Int.* (2003) doi:10.1016/S0272-8842(02)00210-9.

114. Ozeki, K., Aoki, H. & Fukui, Y. Effect of pH on crystallization of sputtered hydroxyapatite film under hydrothermal conditions at low temperature. *J. Mater. Sci.* (2005) doi:10.1007/s10853-005-0420-6.